iJRASET
International Journal For Research in Applied Science and Engineering Technology

INTERNATIONAL JOURNAL FOR RESEARCH

IN APPLIED SCIENCE & ENGINEERING TECHNOLOGY

Volume: 6 **Issue:** III **Month of publication:** March 2018

DOI: http://doi.org/10.22214/ijraset.2018.3263

www.ijraset.com

Call: 08813907089 | E-mail ID: ijraset@gmail.com

International Journal for Research in Applied Science & Engineering Technology (IJRASET)
ISSN: 2321-9653; IC Value: 45.98; SJ Impact Factor: 6.887
Volume 6 Issue III, March 2018- Available at www.ijraset.com

A Comprehensive Review on Chemical Bath Deposited ZnS Thin Film

R. P. Khatri[1], A. J. Patel[2]
[1]*Gujarat Technological University, Chandkheda, Ahmedabad, Gujarat 382424, India*
[2]*Government Engineering College, Godhra, Panchmahal, Gujarat 389001, India*

Abstract: ***Chemical methods for synthesizing metal chalcogenides are currently receiving wide attention because of their simplicity, cost effectiveness and suitability for large scale deposition. Thin films can be deposited on variety of substrate such as insulators, semiconductor or metal because of lower temperature associated with these methods reduces chances of oxidation and corrosion of substrate. Slow release of anions in these processes facilitates better crystallinity with improved grain structure. Depending upon bath parameter, film deposition can take place by ion-ion mechanism of materials on the substrate or adsorption of hydroxide intermediate on substrate. Using these methods, thin films of group II-VI, III-VI, V-VI etc. have been deposited. Photo-sensor, photocells, detectors, photoluminescence, photovoltaic materials, thermo-electric materials, pigments, anti-reflective coating, optical memories, crude petroleum processing etc. are some of the application of metal chalcogenide films.***

In the present review article, we have described brief theoretical background necessary for chemical deposition. We discussed CBD method in details to obtain well-adherent and uniform thin film of ZnS. Their bath parameter, structural, morphological, optical, electrical properties etc. are also described.

Keywords: Chemical bath deposition, Thin films, Metal Chalcogenides

I. INTRODUCTION

Thin films have number of applications in various fields. Few of them are A.R. coating, interference filters, polarizer, narrow band filters, solar cell, photoconductors, IR detectors, wave guide coatings, temperature control of satellites, Photo thermal solar coatings such as black chrome, nickel, cobalt etc., magnetic films, superconducting films, anticorrosive films, microelectronic devices, diamond films, reduction of fabrication though coating or surface modification i.e. epitaxy and heterostructure films, hard coating etc. Rapid growth in film devices has helped for ICs of monolithic and hybrid microelectronics [1].

Metal sulphides have wide range of applications including detector, modulator, and dielectric filter, light emitting diode, efficient phosphor in flat panel display and buffer layer in solar cell [2, 3]. Metal sulphides can protect junction region from deposition or sputtering damage during p-type deposition. These compounds can also modify the surface of solar cell absorbers and reduce the lattice mismatch and difference in band gap energy between n- and p- type layers to obtain high conversion efficiency [4].

Currently Cu (In, Ga)Se_2 (CIGS) (I-III-VI_2 semiconductor) based thin film solar cells with high efficiency have been reported on both laboratory scale and in commercial devices [5]. Although theoretical conversion efficiency of CIGS based thin film solar cell is ~ 30%, maximum experimental efficiency achieved has been approximately ~20% (for small area solar cell) [6]. The CIGS layer has an excellent light absorption co-efficient (10^5 cm^{-1}) and is a better choice for absorber layer than many other materials. In CIGS thin film solar cells, a chemically-deposited CdS buffer layer has been used between the absorber and transparent conductive oxide layers. High conversion efficiency and stability have been achieved with the CdS buffer [7]. However, Cd is carcinogenic and toxic material. As an alternative to CdS buffer, the Cd-free ZnS buffer has been proposed, and research on the ZnS buffer is growing recently [8].

The long wavelength limit in the IR region of the quantum efficiency (QE) spectrum for CIGS solar cell using a ZnS buffer can be blue shifted compare to that for a CIGS solar cell using a CdS buffer. While the poor QE spectrum near blue-green region for CdS-buffered CIGS solar cell is improved in ZnS buffered CIGS cell [8]. The replacement of CdS buffer layers with ZnS buffer layers can decrease absorption losses and improve short circuit current (J_{SC}) in solar cells [9].

This feature is due to large energy band gap of ZnS than ZnO (window) and CdS (3.3 eV [10] and 2.43 eV [11] at room temperature respectively). The ZnS doped with various metals exhibit excellent luminescent properties, when excited by X-rays, ultraviolet rays, cathode rays or electrical current [12-14]. In area of optics, because of its high refractive index (2.35), ZnS is used as a reflector [15]

or as a part of a double layer antireflective coating if used in conjunction with a low refractive index material, and because of high transmittance in the visible range, it is used as a dielectric filter [16].

Several techniques such as molecular beam epitaxy [17], Sputtering [18], MOCVD [19,20], MOVPE [21], PLD [22], electro-deposition [1], or Chemical bath deposition [23] have been used to deposit ZnS thin films. Among these deposition methods, CBD seems to be attractive because it gives a number of advantages over conventional film deposition method. Like all other methods, CBD does not requiring high temperature as well as sophisticated and expensive equipments. Only simple equipements like magnetic stirrer with hot plate is needed. The starting precursors are easily available and cost effective. CBD has large scale capabilities of depositing large number of coat in single run on different substrates. The films can be deposited on different kinds of substrates with various shapes and sizes. Any insoluble surface to which the solution has a free access will be suitable for deposition.

In CBD method, aqueous solution of metal salt (acetate, sulphate, halide etc.) are used as metal precursors. Thiourea, thioacetamide, thiosulphate and sodium sulphide are generally used as sulphide precursors. To control metal ion concentration, complexing agents like hydrazine, ammonia and sodium citrate are used. The reaction takes place in alkaline solution with temperature range 30-90 °C. Uniform and homogeneous films can be obtained with improved grain structures by controlling bath parameters (concentration, pH, temperature etc.). A number of review articles related to CBD are available in literature [1, 24-27].

Formation of solid phase from a solution involves two steps: nucleation and particle growth. Nucleation occurs due to local fluctuation in the solution-whether concentration, temperature or other variable. First stage of growth is collision between individual ions or molecules to form embryos. Embryos grow by collecting individual species colliding with them, resulting into particle of deposit. Without nucleation thin film deposition does not occur. Film formation occurs either by reaction between free anions or by decomposition of metal complex. These two categories are further followed by ion-by-ion mechanism or hydroxide cluster mechanism for film formation.

Using CBD method, large number of binary compounds such as CdS, ZnS, CdSe, ZnSe, Bi_2S_3, Bi_2Se_3, PbS, PbSe, CuS, NiS, Sb_2S_3, As_2S_3, Ag_2S etc. and ternary compounds such as CdZnS, CdPbSe, CdSSe, $CuInS_2$, $CuInSe_2$ etc. have been deposited as thin films.

In the present review article, a survey of ZnS thin films deposited by CBD method is made. Theoretical background of chemical deposition is discussed. Physico-chemical properties of ZnS thin films are summarized.

II. THEORETICAL BACKGROUND OF CHEMICAL DEPOSITION

A. Concept of solubility and ionic product

Consider a very sparingly soluble salt (say ZnS) in equilibrium with its saturated aqueous solution as

$$ZnS_{(s)} \Leftrightarrow Zn^{2+} + S^{2-} \tag{1}$$

Applying law of mass action

$$K = \frac{[Zn^{2+}][S^{2-}]}{[ZnS_{(s)}]} \tag{2}$$

Where $[Zn^{2+}]$, $[S^{2-}]$ and $[ZnS_{(s)}]$ are concentration of Zn^{2+}, S^{2-} and ZnS in solution, respectively. The concentration of pure solid is a constant number i.e. $ZnS_{(s)}$ = Constant = K'

$$K = \frac{[Zn^{2+}][S^{2-}]}{K'} \tag{3}$$

or

$$KK' = [Zn^{2+}][S^{2-}] \tag{4}$$

Since K and K' are constants, the products of KK' is also constant, say K_{sp} therefore equation 4 becomes

$$K_{sp} = [Zn^{2+}][S^{2-}] \tag{5}$$

The K_{sp} is called solubility product and $[Zn^{2+}][S^{2-}]$ is called ionic product. More generally, for the dissolution,

$$M_aX_b \Leftrightarrow aM^{n+} + bX^{m-} \tag{6}$$

$$K_{sp} = [M^{n+}]^a[X^{m-}]^b \tag{7}$$

The precipitation will be formed when the product of the concentrations of anions and cations exceeds the solubility product. From another point of view, phase transformation occurs when the free energy of the new phase is lower than initial phase. There are four main factors which affect the solubility as temperature, solvent, particle size and number of atoms in molecule [28-30]. The direction of solubility changes as a function of temperature. Since increase in temperature by a stress, the equilibrium between precipitate and its ions in solution will shift according to whether the heat of solution is endothermic or exothermic. Using a solvent of lower dielectric constant, the solubility of moderately insoluble substance in water is reduced by the addition of alcohol or some other water miscible solvent. As particle size decreases, the solubility appears to increase. Value of K_{sp} is lower for large number of atoms in molecule (say Bi_2S_3).

Table I represents the values of solubility product at 25 ºC for compound relevant of chemical deposition. It is noteworthy that the deposition of oxides often occurs via a hydroxide or hydrated oxide, and therefore the relevant values of hydroxides are also provided [31].

B. Formation of precipitate in the solution

CD occurs either by initial homogenous nucleation in solution or by hetero-nucleation on substrate depending on deposition mechanism (Fluctuation in the solution; whether in concentration, temperature or other variables). In homogeneous nucleation, collision between individual ions or molecules creates embryos (nuclei). Embryos grow by collecting individual species that collide with them. While these species may be ions, atoms or molecules in general, for CD, adsorption of ions on the embryos

TABLE I
VALUES OF SOLUBILITY PRODUCT (AT 25 °C) FOR COMPOUNDS RELEVANT TO CD

Solid	K_{sp}
Ag_2S	3×10^{-50}
Ag_2Se	10^{-54}
AgCl	2×10^{-10}
AgBr	8×10^{-13}
AgI	10^{-16}
As_2S_3	2×10^{-22}
$Bi(OH)_3$	6×10^{-31}
Bi_2S_3	10^{-100}
Bi_2Se_3	10^{-130}
$Cd(OH)_2$	2×10^{-14}
CdS	10^{-28}
CdSe	4×10^{-35}
CdTe	10^{-42}
$Co(OH)_2$	5×10^{-15}
CoS	10^{-21}

Solid	K_{sp}
FeS	10^{-18}
HgS	6×10^{-53}
HgSe	4×10^{-59}
$In(OH)_3$	6×10^{-34}
In_2S_3	6×10^{-76}
$Mn(OH)_2$	5×10^{-13}
MnS	10^{-13}
$Ni(OH)_2$	3×10^{-16}
NiS	10^{-21}
NiSe	2×10^{-26}
$PbCO_3$	10^{-13}
$Pb(OH)_2$	10^{-15} - 10^{-20}
PbS	10^{-28}
PbSe	10^{-37}
$Sn(OH)_2$	5×10^{-28}

Solid	K_{sp}
CuSe	2×10^{-40}
$Fe(OH)_2$	5×10^{-17}
$Fe(OH)_3$	3×10^{-39}
$Zn(OH)_2$	10^{-16}
ZnS	3×10^{-25}
ZnSe	10^{-27}
Cu_2S	10^{-48}
CuS	5×10^{-36}
SnS_2	6×10^{-57}
SnSe	5×10^{-34}
CuOH	1×10^{-14}
$Cu(OH)_2$	2×10^{-20}
$Sn(OH)_4$	1×10^{-56}
SnS	10^{-26}

seems to be the most probable growth mechanism. In heterogeneous nucleation, subcritical embryos are adsorbed onto substrate. Energy required to form an interface between the embryos and solid substrate will usually be less than that required for homogenous, where no such interface exists. Therefore heterogeneous nucleation is energetically preferred over homogeneous nucleation and occurs near equilibrium saturation conditions compared to homogeneous nucleation, where high degree of supersaturation is required. The nuclei that are subcritical in solution may be supercritical when adsorbed on a substrate. This is a consequence of reduced contact between nucleus and solution as well as stabilization of the adsorbed nucleus. These processes are shown schematically in fig.1.

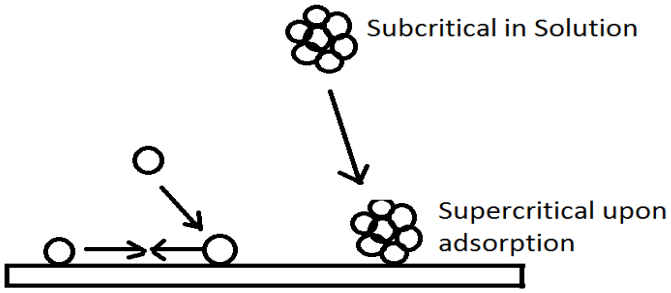

Fig.1 Process involved in heterogeneous nucleation on a substrate

Once nuclei have formed, growth process occurs via various growth mechanisms such as self-assembling process, Ostwald ripening, aggregation or coalescence.

C. Mechanism of chemical Deposition

The mechanism of chemical deposition divided into two categories, formation of the required compound by ionic reactions involving free anions and decomposition of metal complexes. These two categories can be further divided into two types, formation of isolated single molecules that cluster and eventually form a crystal or particle and mediation of solid phase, usually metal hydroxide. The later mechanism also known as ion by ion mechanism and hydroxide cluster mechanism for thin films formation, respectively.

In CD, the trick is to control the rate of reactions so that they occur slowly enough to allow metal chalcogenide either to form gradually on the substrate or diffuse there and adhere either to the substrate itself or to the growing film, rather than aggregate into larger particles in solution and precipitate out. This rate control can be accomplished by generating suphide slowly in the deposition solution which can be controlled to a number of parameter, in particular the concentration of sulphide forming precursor, solution temperature and pH.

D. Reaction Mechanism for ZnS

Formation of ZnS involves following steps:

The alkaline solution containing Zn salt and complexing agent NH_3 which allows for obtaining a soluble species of Zn^{2+} in solution through following reaction [32]:

$$Zn(NH_3)_4^{2+} \rightarrow 4NH_3 + Zn^{2+} \quad (8)$$

Thiourea has been used as S^{2-} source through hydrolysis in alkaline medium:

$$SC(NH_2)_2 + OH^- \rightarrow SH^- + CH_2N_2 + H_2O \quad (9)$$

$$SH^- + OH^- \rightarrow S^{2-} + H_2O \quad (10)$$

And finally zinc sulphide film forms according to reaction,

$$Zn^{2+} + S^{2-} \rightarrow ZnS \quad (11)$$

In the deposition of ZnS film by the above reaction, a competitive process is present in the bath like a source of OH^- through:

$$NH_3 + H_2O \rightarrow NH_4^+ + OH^- \quad (12)$$

But K_{sp} of ZnS is much smaller than $Zn(OH)_2$. Thus sulphide will occur preferentially at surface of hydroxide rather than nucleating separately in solution through reaction:

$$Zn(OH)_2 + S^{2-} \rightarrow ZnS + 2OH^- \quad (13)$$

III. EXPERIMENTAL DETAILS

A. Starting Precursor

B. Zn salt like sulphate, acetate, halide and nitrate etc. are used as Zn precursor. Thiourea, thioacetamide, sodium thiosulphate etc. are used for Sulphur source. Hydrazine hydrates, ethylenediaminetetraacetic acid (EDTA), tri-sodium citrate, Triethanolamine (TEA) etc. are used as complexing agent. Ammonia, NaOH, HCl are used to maintain pH of solution.

C. *Substrate cleaning:* Prior to thin film deposition, substrate has to be cleaned and dried appropriately to improve the adhesion and quality of coating. There are various means suggested by researchers for substrate cleaning and documented in literature [33-37]. The most common includes glass substrate boiled in chromic acid for ~2 hr and kept in it for 12 hr. Then, it is washed with detergent and again rinsed in acetone or methanol. Finally, the substrate is being dried in hot air oven for 1 hr at temperature range 50-100 °C.

D. *Film deposition by CBD method:* Zinc precursor, complexing agent and chalcogenide precursors are used as starting materials. De-ionized water or methanol is generally used as solvent to obtain the precursor solution. First of all, solutions of zinc precursor and complexing agent are mixed and stirred if needed. After the formation of clean and transparent solution, solution of chalcogenide precursor is added slowly under stirring. Then suitable pH is adjusted using NH_3 or NaOH. Pre-cleaned substrate is immersed in prepared solution and kept vertical for thin film deposition. Entire mechanism is kept in water or paraffin bath to maintain constant temperature between room temperature to ~90 ºC for suitably chosen period. Temperature, pH and deposition time depends on optimization of deposition parameter. Finally, substrate is taken out of the reaction bath, washed with de-ionized water and dried in hot air oven. Thickness of film can be increased by reinserting it into freshly prepared solution as mention above [38-40]. Schematic diagram of chemical bath deposition method is presented in fig. 2.

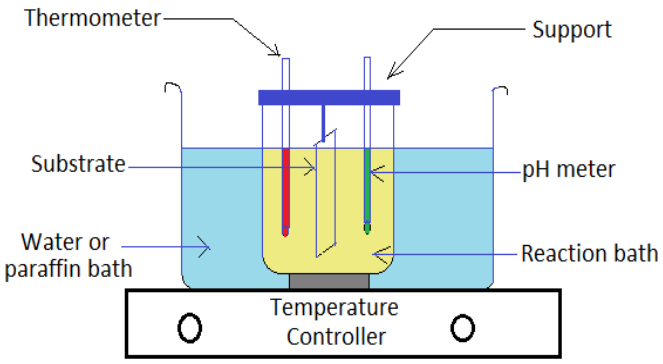

Fig.2 Schematic diagram of Chemical Bath Deposition Method

IV. ZNS FILMS BY CBD METHOD

ZnS thin films prepared by CBD method have been characterized for various properties. Preparative conditions and properties reported in literature are presented in Table II

TABLE II
Preparative conditions and properties of ZnS thin films deposited on various substrates by chemical bath deposition method

No	Film type	Bath Composition	Solvent used	pH Deposition Temp. (ºC) Deposition time	Substrate Film thickness (nm) Film colour	Remarks	Ref.
1	ZnS	$ZnSO_4$+ $SC(NH_2)_2$+ NH_3+ N_2H_4	Distilled water	- 70 ºC 60-90 min	SnO_2/Glass 115-156 -	SEM: Spherical Surface features with surface roughness 34-50 nm.	[41]
2	ZnS	$Zn(CH_3COO)_2$ + $C_6H_{15}NO_3$+ NH_3+ $Na_3C_6H_5O_7$+ $SC(NH_2)_2$	Distilled water	- 80-86 ºC 18 hr to 39 hr	Glass 37 -56 white	Amorphous films band gap: 2.45 - 3.53 eV	[38]

3	ZnS	$ZnCl_2$+ $SC(NH_2)_2$+ NH_3 + N_2H_4	Aqueous+ ethanolic solution (1:10, 1:20, 1:30, &1:40)	9 ± 0.5 70 to 80 ºC –	Glass – Green & pink	Hexagonal structure Activation Energy: 0.66 - 0.96 eV Crystallinity and grain boundary found varying with ethanol concentration	[42]
4	ZnS	$ZnSO_4.7H_2O$/ $Zn(CH_3COO)_2$/ $Zn(NO_3)_2.6H_2O$/ $ZnCl_2$+ $SC(NH_2)_2$+ NH_4OH+ N_2H_4	Distilled water	– 80 ºC 2-5 Hr	Soda lime glass – –	Cubic structure Particle size: 10 nm Surface features: Randomly orientated nanocrystallites Surface roughness: 2.0 - 7.4 nm. Band gap: 3.88 - 3.99 eV. Transmittance: > 85%. Adhesion Strength for as-grown films : 13.3 N - 18 N Adhesion Strength for annealed films: 16 N - 19 N	[43]
5	ZnS	$Zn(CH_3COO)_2$ + $SC(NH_2)_2$ + NH_3+ $Na_3C_6H_5O_7$	Distilled water	9.5- 10.5 82-86 ºC –	Glass – –	Hexagonal Wurtzite structure Particle size: 14 - 18 nm. PL Spectra: Emission of blue region (465 nm)	[44]
6	ZnS:Cu	$Zn(CH_3COO)_2$ + $SC(NH_2)_2$ + NH_3+ $Na_3C_6H_5O_7$ (Post Deposition: ZnS Powder + $CuCl_2$ for doping)	Distilled water	9.5- 10.5 82-86 ºC –	Glass – –	Hexagonal Wurtzite structure In-homogeneous and porous texture observed by SEM. PL Spectra: emission of green region (537 nm).	[44]
7	ZnS:Cu,Mn	$Zn(CH_3COO)_2$+ $SC(NH_2)_2$ + NH_3+ $Na_3C_6H_5O_7$ (Post Deposition: ZnS Powder + $CuCl_2$+ $MnCl_2$ for doping)	Distilled water	9.5- 10.5 82-86 ºC –	Glass – –	Wurtzite and orthorhombic structure PL Spectra: emission of orange region	[44]
8	ZnS:Mn	$Zn(CH_3COO)_2$+ $SC(NH_2)_2$ + NH_3+ $Na_3C_6H_5O_7$ (Post Deposition: ZnS Powder + $MnCl_2$ for doping)	Distilled water	9.5- 10.5 82-86 ºC –	Glass – –	Hexagonal Wurtzite structure PL Spectra: Emission of orange region (578 nm)	[44]
9	ZnS	$Zn(CH_3COO)_2$+ $SC(NH_2)_2$	Distilled water	9-10 30 ºC 18 Hr	Glass 76 - 332 –	Polycrystalline $\rho = 1.832 \times 10^5$ - 0.363×10^5 Ω.cm (at T = 505 K) Activation energy: 0.810 - 1.29 eV	[45]
10	ZnS	$ZnSO_4$+ $SC(NH_2)_2$ + NH_3	Distilled water	– 85 ºC –	Glass 320 –	Amorphous Hexagonal Wurtzite phase Particle size:100 nm Band gap: 3.45 eV $\rho = 0.36 \times 10^5$ Ω.cm at 500 K Activation energy: 0.82 eV.	[46]
11	ZnS	$Zn(CH_3COO)_2$+ $Na_3C_6H_5O_7$+ $SC(NH_2)_2$ +	Distilled water	9.5-10.5 82-86 ºC –	Glass – Milky	Crystalline Wurtzite structure PL Spectra: Emission of green band (~520 nm)	[47]

		NH_3					
12	ZnS:Cu	$Zn(CH_3COO)_2$+ $Na_3C_6H_5O_7$+ $SC(NH_2)_2$ + NH_3 (Post deposition annealing at 500 ºC with Cu ion)	Distilled water	9.5-10.5 82-86 ºC -	Glass - Milky	Crystalline Wurtzite structure Particle size: 14 nm Transmittance: 70% for Zn and Cu molar ratio 1:3. PL Spectra: Emission of green region	[47]
13	ZnS:Cu,Mn	$Zn(CH_3COO)_2$+ $Na_3C_6H_5O_7$+ $SC(NH_2)_2$ + NH_3 (Post deposition annealing at 500 ºC with Cu-Mn ion)	Distilled water	9.5-10.5 82-86 ºC -	Glass - Milky	Crystalline Wurtzite structure Particle size: 14 nm PL Spectra: Emission of Blue region (~488 nm) (for direct doping) and orange- red emission (~578 nm) (for Indirect doping).	[47]
14	ZnS	$ZnSO_4$+ $SC(NH_2)_2$	Distilled water	- 85 – 150 ºC 30 min & 80 min	Glass - -	Hexagonal structure Particle size: 320 nm Band gap: 3.54 and 3.49 eV Absorption edge at 286 nm. PL Spectra: Green emission (for 500 nm) and Violet emission (for 427 nm).	[48]
15	ZnS	$ZnSO_4$+ $SC(NH_2)_2$+ NH_4OH	Distilled water	- 70 ºC -	Glass 73 - 91 -	Particle size: 152 - 202 nm. Band gap: 4.05 - 3.99 eV. Transmission: 95% - 99%.	[49]
16	ZnS:Cu	$ZnCl_2$ + EDTA+ $C_6H_{15}NO_3$+ NH_4OH+ $CuCl_2.2H_2O$	Distiiled water	10.1 - -	Glass 670 -	Uniform & transparent films Band gap: 2.40 - 2.70 eV Extinction coefficient: between 6.6 × 10^{-2} and 8 × 10^{-5} Refractive index = 1.0 to 2.60	[50]
17	ZnS:Cu	$Zn(CH_3COO)_2$+ Na_2EDTA+ C_2H_5NS + $CuSO_4$	Deionized water	- 80 ºC 3 Hr	Glass - -	P-type films Cubic or β-ZnS structure Band gap: 3.8 - 3.70 eV Transmission: 60% to 80%. Sheet Resistance = 1.73 × 10^5 to 8.5 × 10^4 Ω.cm^{-2}.	[51]
18	ZnS:Ni	$Zn(NO_3)_2$+ $Ni(NO_3)_2$+ NH_4NO_3+ $Na_3C_6H_5O_7$+ $SC(NH_2)_2$	Deionized water	11 80 ºC 30 min - 2 hr	ITO 72 - 237 Bright silvery (ZnS) Yellowish (ZnS:Ni)	Conductivity changes from n-type to P-type at higher Ni doping. SEM: Hierarchical structure with rod like branches (for ZnS) and small densely packed aggregates (for ZnS:Ni). Elemental ratio: 56.13 at% of Zn, 43.46 at% of S and 0.41 at% of Ni. Transmittance: ~ 55 % in range 475 - 575 nm Band gap: 3.37 - 3.02 eV Carrier Concentration: 2.82 ×10^{14} to 1.29 × 10^{14} cm^{-3} Photo current density = 0.82 and 3.74 mA/cm^2 (for Ni, x=0.005 and 0.003)	[52]
19	ZnS	$ZnSO_4.7H_2O$+ $C_6H_{15}NO_3$+	Deionized water	- -	Glass -	Amorphous films, Little crystalline on annealed at 500°C.	[39]

		NH_4Cl+ $Na_3C_6H_5O_7$ + C_2H_5NS		24 hr	light green	Transmission: 75 % to 45 % (with thickness variation) and 58 % to 26 % (with temperature variation). Extinction coefficient: 0.33 - 0.99 Refractive Index: 1.97 - 2.69 Conductivity: 1.49 × 10^{-9} to 9.14 × 10^{-10} Ω $^{-1}$.cm $^{-1}$ Raman phonon mode at ~478 cm^{-1}, ~778 cm^{-1} and ~1082 cm^{-1}. Energy difference for Raman spectrum: 0.0593 - 0.1342 eV. Real part of dielectric constant: 3.60 - 4.69 Imaginary part of dielectric constant: 1.64 - 4.58 Reverse saturation current: 2.650×10^{-15} - 1.31×10^{-14} A Zero bias apparent barrier height: 1.076-1.131 eV Ideality factor = 2-10	
20	ZnS:PbS Zn/Pb = 1% - 5%	$ZnCl_2$+ NaOH+ $SC(NH_2)_2$+ $Pb(NO_3)_2$	Deionized water	12 25 ºC –	Glass 400 –	Polycrystalline cubic phase (a= 0.2986 Å to 0.2967 Å) Particle size: 13 - 39 nm. AFM: Uniform and dense surface, Surface roughness: 60-73.4 nm Band gap: 0.72 - 1.46 eV, Transmission: 35 % to 75 % Absorption coefficient: 10^3 cm $^{-1}$ Extinction coefficient: 0.01 - 0.3, Refractive Index: 1.6 to 2.6 Resistivity: 0.28 to 691.1 Ω.cm Carrier Concentration: 4.31 x 10^{17} - 1.15 x 10^{15} cm^{-3} Micro strain: 0.8885 x 10^{-5} - 2.5761 x 10^{-5} Dislocation density: 0.6575 x 10^{15} - 5.5278 x 10^{15} lines/cm^2	[53]
21	ZnS	$ZnSO_4.7H_2O$+ $C_4H_6O_4$+ NH_3 + N_2H_4+ $SC(NH_2)_2$	Double Distilled water	10.7 5 ºC 9 hr	Glass – –	Hexagonal structure with a= 3.71 Å and c = 25.271 Å Globular structure with densely packed grain observed by SEM Av. Crystallite size = 17 nm, Av. Grain size = 18.4 nm n-type films Conductivity: 10^{-5} at R.T. & 2 x 10^{-5} - 5.49 x 10^{-2} (T=300 K-525 K) Transmittance: 60%, Activation energy: 0.082 and 0.54 eV.	[54]
22	ZnS:Al	$Zn(CH_3COO)_2$+ Na_2S+ $Al_2(SO_4)_3$+ NH_3+ N_2H_4	Methanol+ Distilled water	5.8 75 ºC 60 min	Glass – Yellow or pale yellow	Polycrystalline zinc bland phase, grain size: 8 to 15 nm Elemental ratio: 44.09 at% of Zn, 49.8 at% of S and 7.4 at% of Al. Transmittance: 75%, Band gap: 3.54 - 3.76 eV N-type films, ρ = 10^7 - 10^3 Ω.cm.	[40]

						FTIR: Strong absorption peak at 1630 cm^{-1} and 3420 cm^{-1}.	
23	ZnS	$ZnSO_4$ + $SC(NH_2)_2$ + NH_3 + $Na_3C_6H_5O_7$	Deionized Water	- 60 - 80 ºC -	Glass - -	Wurtzite structure Band gap: 3.7 and 4.05 eV Absorption edge at 330 nm EDAX: Zn = 38.2 at% & S = 61.8 at%	[55]
24	ZnS	$Zn(CH_3COO)_2$ + $Zn(NO_3)_2$ + $ZnSO_4$ + $SC(NH_2)_2$ + NH_4OH + $Na_3C_6H_5O_7$	Distilled water	- 80 ± 1 ºC -	Si_3N_4 50 (for ZnAc) 50 (for $ZnSO_4$) 60 (for $Zn(NO_3)_2$) -	Amorphous (disordered materials) nature of films. SEM: discontinuous film with some ZnS cluster formation (for ZnAc), A few pinholes but no clusters (for $ZnSO_4$), Uniform free from pin holes and cluster (for $Zn(NO_3)_2$) with surface roughness ~ 5 nm (ZnAc) ~ 3 nm : ($ZnSO_4$ & $Zn(NO_3)_2$), respectively. Band gap: 3.72 eV (for ZnAc) & 3.71 eV (for $Zn(NO_3)_2$). XPS: Zn 2p3 binding energy between 1022.6 eV to 1021.7 eV related to Zn-OH and Zn-S bond, respectively. S 2p binding energy observed at 161.7 eV and at 162.2 eV for Zn-S bonding.	[56]
25	ZnS	$Zn(CH_3COO)_2$+ $SC(NH_2)_2$ + NH_3	Distilled water	9 to 10 30 ºC -	Glass 76 to 332 White	XRD: Polycrystalline Hexagonal structure. Crystallinity of films increase with thickness. Electrical resistivity: 1.832 $\times 10^5$ - 0.363 $\times 10^5$ Ω·cm Activation energy: 0.81 - 1.29 eV.	[57]
26	ZnS	$Zn(CH_3COO)_2$+ $SC(NH_2)_2$ + NH_3	Distilled water	11.0 80 ºC 3 hr	ZnO nanowire coated glass - -	No diffraction peaks observed for XRD. SEM: ZnS coating is confirmed. TEM: ZnS coating is confirmed on ZnO nanowire. Transmission: 38 % (for 1 Hr) and 9 % (for 3 hr) at 500 nm. PL spectra: Peak at 380, 550 and 680 nm (for 1 hr) and additional peak at 420 nm (for 3 hr). J-V Characteristics: V_{oc}=0.45 mV, J_{sc}= 0.40-1.84 (mA/cm^2), fill factor = 29.54-37.05, η = 0.07-0.24%	[58]
27	ZnS	$Zn(CH_3COO)_2.2H_2O$ + C_2H_5NS + HCl + $C_2H_8N_2$	Deionized water	- - -	p- type Si (100) - -	XRD: Polycrystalline films with dominant cubic phase over small amount of hexagonal phase, grain size 11.5-14.5 & 18.0-25.0 nm respectively. SEM: Hemispherical structure composed of agglomerated particles (without En) and smoother and compact; continuous uniformity and the absence of	[59]

						agglomerated particles (With En). E_g varied from 3.35 to 3.75 eV. PL showed blue shift with increasing En, Excitation wavelength at 310 nm and wide light emitting band in visible region.	
28	ZnS	$Zn(en)_3SO_4$ + $CS(NH_2)_2$ + NaOH + or $Zn(trien)(ClO_4)_2$ + $CS(NH_2)_2$ + NaOH (en: ethylenediamine) (trien: triethylenetetraamine)	Distilled water	12.7 to 13.5 60 ºC 10 hr	Polyethelene and Glass - Colourless	Low Crystallinity and Sphalerite structure. SEM: Fairly uniform particle size <1 mm (for film A) & Large cracks; probably due to separately grown colonies of accumulations. EDAX: Zn/S ratio = 2.2:1.0 (for A) & 2.0: 1.0 (for B). Transmission: 90 % at a wavelength of 1000 nm, down to 15 % at 400 nm. PL spectra: Emission peaks at 450 and 485 nm.	[60]
29	ZnS:Al	$ZnSO_4.7H_2O$ + $SC(NH_2)_2$ + NH_4OH+ $(NH_2)_2.H_2O$	Distilled water	- 80 ºC -	Glass 224 - 347 -	Monocrystalline, Sphalerite, β-ZnS with preferentially oriented along (111), Crystal size: 12 to 17 nm. Band gap: 3.65-3.87 eV. Transmission: 75 % in VIS & NIR range. PL spectra: Emission peaks at 365 nm, 420nm, 484 nm, 528 nm and 600 nm. Raman Spectroscopy: Peak at 260, 343, 424, 652 and 950 cm^{-1}. Extinction coefficient: η_{mass} = 2.30 to 2.33, $\eta_{H\text{-}V}$ = 2.12 to 2.17 and $\eta_{Ravindra}$ = 1.68 to 1.82. Single Oscillator energy(E_0): 5.85 to 10.42 eV, Dispersion energy (E_d) = 20.85 to 10.11 eV, Urbach energy (E_u) = 0.42 to 0.31 eV Carrier concentration to the effective mass ratio (N/m*) = 2.22 to 4.87 × 10^{47} kg/cm^3	[61]
30	ZnS	$Zn(CH_3COO)_2$+ $SC(NH_2)_2$+ NH_3	deionized water	9 to 10 30 ºC 17 - 20 hr	Glass 330 nm (17 hr, 30 °C) 310 nm (20 hr, 45 °C) -	XRD: Polycrystalline hexagonal structure with particle size ranging 6.9 to 17.8 nm. Deposition rate increases with NH_3 concentration. N-type conductivity. Band gap: 3.68 - 4.10 eV.	[62]
31	ZnS	ZnSO4 + $SC(NH_2)_2$ + NH_3	Distilled water	- 90 ºC -	Soda lime glass - -	XRD: Cubic structure with (111) preferential direction. Amorphous at 100 ºC annealed temperature and crystalline at higher temperature.	[63]

						SEM: Large grains and pinholes on the surface (annealed at 100 °C) and uniform, granular structure at high temperature annealing. AFM: Annealed films composed of clusters, compact, smooth surface with roughness 28.49 to 19.91 nm. Transmittance: 70% - 80% in visible region. Band gap: 3.89 - 3.82 eV.	
32	ZnS	$(CH_3COO)_2.2H_2O$ + $Na_2S.9H_2O$	Distilled water	- 80 ºC -	Glass - -	Preferred orientation along (200), Particle size: 27 nm. Zn rich atomic concentration. PL spectra: Peak at 434, 468, 488, 387 and 449 nm for (λ_{ex} = 356 nm) and CIE diagram emission colour is blue. Additional peaks originated at 343 and 365 nm (for λ_{ex} = 245 nm) Band emission is bluish white colour.	[64]
33	ZnS	$ZnCl_2$ + CH_4N_2O + C_2H_5NS + HCl	Deionized water	4 80 ºC 3 hr	Glass 5000 -	XRD: Cubic phase with a = 5.32 Å. TEM: Good crystallinity with d = 0.3 Å. AFM: Uniform and smooth surface with RMS roughness 0.4231 nm and average roughness 0.3201 nm. Transmission: 70-90 % in visible region. Band gap: 3.78 eV. PL spectra: Green emission at 555 nm.	[65]
34	ZnS	$ZnSO_4.7H_2O$ + $SC(NH_2)_2$ + NH_4OH	Deionized water	- 80 ºC 40 min	bare glass & ITO coated glass - -	XRD: Polycrystalline cubic structure. Crystallite size 32-46 nm (bare), 40-57 nm (A-bare), 30-54 nm (ITO), 35-76 nm (A-ITO). Sharp absorption edge. Higher transmittance above 700 nm. N-type conductivity.	[66]
35	ZnS	$Zn(CH_3COO)_2$+ $SC(NH_2)_2$ + $Na_3C_6H_5O_7$+ NH_4OH	Deionized water	- 80 ºC 15 - 75 min	Glass 70 - 85 -	XRD: Hexagonal polycrystalline film. XPS: Zn-S bonding energy is 1022.5 and 162.1 eV for Zn 2p3/2 and S 2p1/2 respectively. Transmittance: 90 % from near ultraviolet to near infrared region. Absorption edge at 310 nm. Band Gap: 3.76 eV, 3.74 eV & 3.71 eV.	[67]
36	ZnS	$ZnSO_4.7H_2O$ + $SC(NH_2)_2$ + NH_4OH + $N_2H_4.H_2O$	Deionized water	- 50-90 ºC 2 - 2.5 hr	Glass 90- 160 -	XRD: Cubic structure. SEM: Continuous and homogeneous film surface. Zn/S ratio: 1.39 to 1.25. Transmittance: Greater than 90 % for visible region. Band gap: 3.93 - 4.06 eV.	[68]

37	ZnS	$Zn(CH_3COO)_2$+ $SC(NH_2)_2$ + $Na_3C_6H_5O_7$+ EDTA + NH_4OH	Deionized water	10 80 ºC 4 hr	Glass 50 - 130 -	SEM: Uniform, continuous and dense microstructures consisting very small sized grains (30-100 nm). XPS: Zn $3p_{3/2}$ binding energies between 1021.9 eV and 1022.6 eV and S 2p binding energies at 161.8 eV and 163 eV, respectively. Transmittance: 65%, 70% and 85% for different complexing agent. Absorption edge near 300 nm for all films with band gap between 3.94 to 3.84 eV. ρ: 1.69 $\times 10^5$ - 1.74 $\times 10^6$ Ω·cm, Mobility: 2.23-5.98 $cm^2/V{\cdot}s$ Carrier Concentration: 0.962 $\times 10^9$ to 9.12 $\times$ 10^{10} cm^{-3} N-type conductivity	[69]
38	ZnS	$ZnSO_4$ + N_2H_4 + NH_3 + $SC(NH_2)_2$	Deionized water	- 70 ºC 2 hr	Glass - -	XRD: Zinc blende structure. Optimal condition for deposition of high quality films: 0.75 M Thiourea concentration and NH_3/N_2H_4 ratio of 0.8 - 1.2 M. SEM: TU has no obvious effect on the surface morphology and ammonia concentration has obvious effect on surface morphology. EDS: Zn (at %) = 33.47 to 44.13 and S (at %) = 65.48 to 55.87. Transmittance: above 70% band gap: 3.76-3.87 eV.	[70]
39	ZnS	$Zn(CH_3COO)_2$+ C_2H_5NS + Na_2EDTA + NH_3	Deionized water	5 - 6.5 80 ºC 4 hr	Glass 30 to 220 -	XRD: Hexagonal structure. SEM: Smooth pinhole free, continuous, uniform surface, Non-agglomerated particle (for pH = 5 - 5.5) and a hemispherical structure agglomerated grains of 100 nm (for pH = 6 -6.5). XPS: binding energies of Zn $p_{3/2}$ between 1021.7 eV and 1022.1 eV & binding energies of S 2p at 160.5 eV and 162.2 eV. Transmittance between 70% and 85% and sharp absorption edge at 300 nm with band gap 3.86-3.91 eV.	[71]
40	ZnS	$Zn(CH_3COO)_2$ + $C_6H_{15}NO_3$ + NH_3/NH_4Cl + $Na_3C_6H_5O_7$+ $SC(NH_2)_2$	Deionized water	10.55 80 ºC 3 - 4.5 hr	Glass 403 - 934 pink & green	XRD: polycrystalline Hexagonal structure, with preferential orientation along (008), a=0.386 nm, c=2.43 nm and crystallite size 40-82 nm. EDS: S/Zn ratio between 0.56 and 0.58.	[72]

						Transmittance: 66 to 87 % in visible region, Band gap: 3.79 to 3.93 eV, Dark resistivity = 2.14×10^{9} Ω.cm, Conductivity = 4.67×10^{-10} Ω^{-1}.cm^{-1}, Carrier Conc. = 1×10^{7} cm^{-3}.	
41	ZnS	$Zn(CH_3COO)_2.2H_2O$ + C_2H_5NS + Na_2EDTA + $C_6H_{12}N_4$	Deionized water	4 80 ºC 2 hr	Glass 37 - 135 –	XRD: Hexagonal structure. SEM: ZnS buffer layer with continuous and uniform morphology deposited on CIGS absorber layer. Nano-sized grain as well as particle shaped grains with roughness decreases from 10 to 2.6 nm with increasing HMTA quantity. EDS: Zn rich film for higher HMTA. Absorption edge at 290 nm. Transmittance: 70% to 80% Band gap: 3.75 - 3.87 eV, Resistivity = 2.4×10^{4} Ω·cm, Conductivity: N-type, Mobility = 4.28 cm^2/V.s Carrier Concentration = 6.09×10^{10} cm^{-3}.	[73]
42	ZnS	$Zn(CH_3COO)_2$+ $SC(NH_2)_2$ + NH_3 + $Na_3C_6H_5O_7$	Deionized water	10 80 ºC 4 hr	Glass 140 - 70 –	XRD: Hexagonal structure. SEM: Non uniform surface with aggregation of different shape and size grains into bigger flat grain (for 0 M Na_3citrate) and densely packed small grains, free from pinholes and display homogeneity (for 0.2 M Na_3citrate). AFM: rough surface (0 M Na_3citrate) and smooth surface with decrease in rms value (0.2 M Na_3citrate). XPS: binding energies at 1022.3 eV and 1022.5 eV for $Zn2p_{3/2}$ and 161.9 and 162.5 eV for $S2p_{1/2}$.	[74]
43	ZnS	$Zn(CH_3COO)_2$+ $Na_3C_6H_5O_7$+ $SC(NH_2)_2$ + NH_4OH	Deionized water	10.0 - 10.75 80 ºC 90 min	SiO_2 50 - 55 –	XRD: Hexagonal structure. SEM: Non homogeneous surface and formation of small agglomerates (pH: 10), poor uniformity and irregular grains are uniformly distributed (pH: 10.25), more homogeneity, free of agglomerates (pH: 10.75). Transmittance: between 75 to 90 % Band gap: 3.68 - 3.73 eV. Resistivity: 1×10^{7} Ω.cm	[75]
44	ZnS	$ZnSO_4$ + N_2H_4/ $Na_3C_6H_5O_7$+ NH_3 +	Deionized water	– 70 ºC 2 hr	Glass 80 to 300 –	Films grown using hydrazine hydrate as complexing agent are composed of denser and smaller particles than those grown using	[76]

		$SC(NH_2)_2$				Na_3citrate. ED: Zn rich film with S/Zn ratio = 0.55-0.94 (for Na_3citrate) and 0.58-0.79 (for hydrazine hydrate). Transmittance: 75 % in visible region Band gap: 3.72-3.87 eV (for Na_3citrate) and 3.74-3.88 eV (for HH).	
45	ZnS	$ZnSO_4$ + NH_4OH + $SC(NH_2)_2$	Deionized water	- 75 – 95 ºC 2 hr	Glass 73 - 200 -	XRD: as-deposited and annealed films are amorphous. Transmittance: 75% for λ above 600 nm. Transmittance of annealed film is lower than that of as-deposited film. SEM: Large particles exist on the small grain-packed surface, more and more large particles appear with increasing deposition temperature.	[77]
46	ZnS	$Zn(CH_3COO)_2.2H_2O$ + $Na_3C_6H_5O_7$ + Na_2EDTA + $SC(NH_2)_2$ + NH_4OH	Deionized water	10 80 ºC 4 hr	ITO/ glass 100 -	XRD: amorphous and poor crystalline structure (for as-deposited, annealed under vacuum & N_2 atm.) and sharp peak of cubic ZnS (for annealed under N_2 + H_2S atm.). XPS: binding energies Zn 2p of as-deposited film at 1022 eV and 1022.7 eV and annealed film at 1022.9 eV; S 2p binding energies at 162 eV and 163 eV for as-deposited and annealed film, respectively. Elemental ratio was near stoichiometric (for as-deposited & vacuum annealed) and poor in Zn and rich in S (N_2+H_2S annealed) films. Absorption edge occurs at 290-310 nm range. Band gap: 3.5 to 3.9 eV.	[78]
47	ZnS	$ZnSO_4$ + $SC(NH_2)_2$ + NH_3	Deionized water	- 80 ºC -	Glass 120 - 140 -	Films were discontinuous (for Non-film phase) and compact and granular structure with grain size 100 nm (for quasi-linear). Transmission was 90% in visible region with band gap 3.51 eV. XPS revealed large amount of oxygen.	[79]
48	ZnS	$ZnSO_4/ZnI_2$ + $SC(NH_2)_2$ + NH_4OH	Deionized water	- 60 – 80 ºC -	quartz 200 -	Surface feature showed crack developed on the surface (one step growth); an assembly of minute particles with cracks (two step growth). Absorption edge occurred at 337	[80]

						nm (for one step growth process & self-catalyst growth process); No clear absorption edge (for two step process)	
49	ZnS	$ZnCl_2$/ $ZnSO_4.7H_2O$/ $Zn(NO_3)_2$/ $Zn(CH_3COO)_2.2H_2O$ + $CO(NH_2)_2$/ C_2H_5NS + NaOH/HCl	Deionized water	5.9 - 6.1 80 ºC 4 hr	Glass 133 - 175 –	Crystallinity increases with annealing at 500 °C under Ar/H_2S environment. Band gap decrease with increase in thickness of film from 3.83 to 3.66 eV. SEM: Particle size of film deposited by zinc acetate is bigger than other film deposited by various Zn salt; compact and no pinhole (for $ZnCl_2$ & $ZnSO_4$). Raman Spectra: Small peak positioned at 355 cm^{-1}. Zn/S ratio is close to optimum stoichiometric and slightly excess in Zn rich for ZnAc.	[81]
50	ZnS	$ZnSO_4$ + $SC(NH_2)_2$ + NH_4OH	Deionized water	- 80 ºC 1 -3 hr	Glass 50 - 207 –	Amorphous structure. Transmission: 85% and decreases with increasing deposition time. Band gap: 3.72 - 3.9 eV. Infinite sheet resistance.	[82]
51	ZnS	$ZnCl_2$ + $Na_2S_2O_3$	Deionized water	2 to 4 85 ºC 10 min	Glass, FTO, Ti, 100 - 500 –	Non-uniform and powdery films. Electrical resistivity: 10^6 - 10^7 Ω·cm Band gap: 3.40 eV.	[83]
52	ZnS	$Zn(CH_3COO)_2$+ C_2H_5NS + N_2H_4+ NH_4Cl	Deionized water	alkaline – –	Glass – –	Band gap: 3.6 - 4.0 eV.	[84]
53	ZnS	$ZnCl_2$+ $C_6H_{15}NO_3$+ NaOH+ $SC(NH_2)_2$	Deionized water	8 to 9 27 -60 ºC 8 hr	Glass & Quartz100 –	Growth of ZnS films depends on bath temperature	[85]
54	ZnS	$ZnSO_4$+ C_2H_5NS + $C_6H_{15}NO_3$	Deionized water	10 75 ºC 36 hr	Glass 440 –	Various films Cu_xS, Bi_2S_3, PbS were deposited on ZnS films and improvement in solar control coating and solar absorption was obtained.	[86]
55	ZnS	$ZnCl_2$+ N_2H_4+ $SC(NH_2)_2$	Deionized water	alkaline – –	Glass – –	Band gap: 3.5 eV.	[87]
56	ZnS	$Zn(CH_3COO)_2$+ N_2H_4+ $C_6H_{15}NO_3$+ $SC(NH_2)_2$	Deionized water	alkaline 25 ºC –	Glass – –	Band gap: 3.7 - 3.8 eV.	[88]
57	ZnS	$ZnSO_4$+ NH_3+ N_2H_4+ $SC(NH_2)_2$	Deionized water	10 – –	Glass – –	Cubic structure Band gap: 3.6 eV	[89]

58	ZnS	$ZnSO_4$+ $SC(NH_2)_2$+ $NH_2.NH_2$	Deionized water	11.5 70 ºC 80 -120 min	Glass 60 -	Microcrystalline films with cubic structure. SEM: continuous and homogeneous films. Resistivity: 10^9 Ω·cm Band gap: 3.76 eV.	[90]

V. CONCLUSION

In the present review article, we have described theoretical background for chemical bath deposition of ZnS thin films. ZnS film formation occurs via heterogeneous nucleation rather than homogeneous nucleation. This method is simple, cost-effective and suitable for large scale deposition and capable of depositing well adherent and good quality ZnS thin film. ZnS thin films have been successfully grown using variety of precursor materials (i.e. $ZnCl_2$, $Zn(CH_3COO)_2$, and $ZnSO_4$ as Zn source; and Thiourea, Thioacetamide and Na_2S as sulphur source). Large variety of complexing agents (i.e. urea, ethylenediamine, Dimethyl Oxalate, Hexamethylenetetramine, Triethanolamine, EDTA, Hydrazine Hydrate, Na_2EDTA, Sodium Citrate, Sodium Hydroxide, Ammonia, Ammonium Chloride, Ammonium Hydroxide and Ammonium Nitrate) are successfully used to synthesize ZnS thin films having variety of structural, morphological, optical and electrical properties. Data presented in tabular form indicate that the film formation carried out onto various substrates (glass, quartz, ITO, ZnO nanowires, Si_3N_4, SiO_2, Polyethelene, FTO). The physico-chemical properties of ZnS are comparable with ZnS prepared by other methods. Simple procedure, requirement of low cost precursors and relatively low temperature requirement associated with chemical bath deposited ZnS thin film make it an optimistic way to prepare the devices such as solar cells, light emitting diode, chemical/ biological sensors, photo-catalysis, flat panel display etc. in modern thin film technology.

VI. ACKNOWLEDGEMENT

The authors are grateful to Prof. M. P. Deshpande, Prof. G.K. Solanki and Prof. S.H. Chaki, Department of Physics, Sardar Patel University, Vallabh Vidhayanagar, Gujarat, India for providing their kind support and guidance.

REFERENCES

[1] R. S. Mane, C. D. Lokhande, Materials Chemistry and Physics, vol. 65, pp. 1-31, 2000.
[2] Nakamura S., Yamada Y., Taguchi T., J. Cryst. Growth, vol. 214, pp. 1091-1095, 2000.
[3] Elidrissi B., Addou M., Regragui M., Bougrine A., Mater. Chem. Phys., vol. 68, pp. 175-179, 2001.
[4] I. Oladeji, L. Chow, J. Liu, W. Chu, A. Bustamante, C. Fredricksen and A. Schulte, Thin Solid Films, vol. 359, pp. 154, 2000.
[5] L. Qj, and G. Mao, Appl. Surf. Sci., vol. 254, pp. 5711, 2008.
[6] S. N. Kundu, S. Johnston, and L. C. Olsen, Thin Solid Films, vol. 515, pp. 2625-2631, 2006.
[7] I. Repins, M. A. Contreras, B. Egaas, C. DeHart, J. Scharf, C. L. Perkins and R. Noufi, Prog. Photo-volt: Res. Appl., vol. 16, pp. 235, 2008.
[8] T. Nakada, M. Hongo, and E. Hayashi, Thin Solid Films, vol. 431-432, pp. 242-248, 2003.
[9] R. N. Bhattacharya and M. A. Contrearas, J. Appl. Phys., vol. 43, pp. L1475, 2004.
[10] U. Ozgur, Y. I. Alivov, C. Liu, A. Teke, M. A. Reshchikov, S. Dogan, Appl. Phys. Rev., vol. 98, pp. 041301, 2005.
[11] B. Ulrich, R. Schroeder, W. Graupner and H. Sakai, Optics Express, vol. 9, pp. 116, 2001.
[12] Qi L., Lee B.I., Kim J.M., Jang J.E., Choe J.Y., J. Lumin., vol. 104, pp. 261-266, 2003.
[13] Wang Z., Daemen L.L., Zhao Y., Zha C.S., Downs R.T., Wang X. and Hemley R.J., Nat. Mater., vol. 4, pp. 922 – 927, 2005.
[14] Corrado C., Jiang Y., Oba F., Kozina M., Bridges F., Zhang J.Z., J. Phy. Chem., vol. 113, pp. 3830-3839, 2009.
[15] Borah J.P., Sarmak C., Acta Phys. Pol. A, vol. 114, pp. 713-719, 2008.
[16] Zhang G., Zhao J., Green M.A., Sol. Energy Mater. Sol. Cells, vol. 51, pp. 393-400, 1998.
[17] J.P. Bosco, S.B. Demers, G.M. Kimball, N.S. Lewis, H.A. Atwater, Journal of Applied Physics, vol. 112 (9), pp. 093703-1-6, 2012.
[18] D.H. Hwang, J. H. Ahn, K. N. Hui, Y. G. Son, Nanoscale Res. Lett., vol. 7:26, pp. 1-7, 2012.
[19] P. J. Dean, A.D. Pitt, M.S. Skolnick, P.J. Wright, B. Cockayne, Cryst. Growth, vol. 59, pp. 301, 1982.
[20] O. Briot, N. Briot, A. Abounadi, B. Gil, T. Clorite, R. Aulombard, Semicond. Sci. Technol., vol. 9, pp. 207-209, 1994.
[21] Dean P.J., Pitt A.D., Skolnick M.S., Wright P.J., Cockayne B., J. Cryst. Growth, vol. 59, pp. 301-306, 1982.
[22] Luo P.F., Jiang G., Zhu C., Chin. J. Chem. Phys., vol. 22, pp. 97-101, 2009.
[23] P. O'Brien, and J. McAleese, Mater. Chem., vol. 8, pp. 2309, 1998.
[24] C.V. Suryanarayana, Bull. Electrochem., vol. 2 , pp. 57, 1986.
[25] C. Cruz-Vazquez, F. Rocha-Alonzo, S.E. Burruel-Ibarra, M. Barboza, R. Barnal, M. Inoue, Appl. Phys. A, vol. 79, pp. 1941-1945, 2004.
[26] H. Ahn and Y. Um, J. of the Korean Phys. Soc., vol. 67(6), pp. 1045-1050, 2015.
[27] H. J. Zhu, X. M. Wang, X. Y. Gao, J. of the Korean Phys. Soc., vol. 67(2), pp. 366-370, 2015.
[28] D.J. Pietrzyk, C.W. Frank, Analytical Chemistry: an Introduction, Academic Press, New York, 1974.
[29] D.A. Skoog, D.M. West, Fundamentals of Analytical Chemistry, 2nd Edition, Holt, Rinehart & Winston, New York, 1980.
[30] .D.A. Skoog, D.M. West, Analytical Chemistry: an Introduction, 3rd Edition, Holt, Rinehart & Winston, New York, 1979.

[31] Gary Hodes, Chemical Solution Deposition of Semiconductor Films, Marcel Dekker, New York, 2002.
[32] J. Vidal, O. Vigil, O. de Melo, N. Lopez, O. Zelaya-Angel, Mater. Chem. Phys., vol. 61, pp. 139-142, 1999.
[33] Xin Yu, Cao Li-yun, Huang Jian-feng, Liu Jia, Fei Jie, Yao Chun-yan, J. of Alloys and Comp., vol. 549, pp. 1-5, 2013.
[34] Rahul Vishwakarma, J Theor. Appl. Phys., vol. 9, pp. 185-192, 2015.
[35] M. Dhanasekar, G. Bakiyaraj, K. Rammurthi, Inter. J. of Chemtech Res., vol. 7(3), pp. 1057-1064, 2014-15.
[36] M. Ashok Kumar and S. Muthukumaran, J. Mater. Sci: Mater Electron, vol. 24, pp. 2858-2865, 2013.
[37] DongBo Fan, Hao Wang, YongCai Zhang, Jie Cheng, Bo Wang, Hui Yan, Mater. Chem. and Phys., vol. 80, pp. 44-47, 2003.
[38] Huda Abdullah, Norhabibi saadah and Sahbuddin Shaari, World Appl.Sci. Journal, vol. 19(8), pp. 1087-1091, 2012.
[39] F. Gode, Physica B, vol. 406, pp. 1653-1659, 2011.
[40] K.Nagamani, P. Prathap, Y. Lingappa, R.W. Miles and K.T.R. Reddy, Physics Procedia, vol. 25, pp. 137-142, 2012.
[41] T. Ben Nasr, N. Kamoun, C. Guasch, Material Chem. and Phys., vol. 96, pp. 84-89, 2006.
[42] Serap Sur, Zihni Ozturk, Mustafa Oztas and Metin Bedir, Phys. Scr., vol. 82, pp. 045604, 2010.
[43] Tingzhi Liu, Huan Ke, Hao Zhang, Shuwang Duo, Qi Sun, Xioyan Fei, Guyue Zhou, Materials Science in Semiconducting Processing, vol. 26, pp. 301-311, 2014.
[44] Maria Stefan, Elisabeth-Jeanne Popovici, Ovidiu Pana, Emil Indera, Journal of Alloys and Compound, vol. 548, pp. 166-172, 2013.
[45] A U Ubale and D K Kulkarni, Bull. Mater. Sci., vol. 28, pp. 43-47, 2005.
[46] M. S. Shinde, P.B. Ahirrao, R.S. Patil, Archives of Applied Science Research, vol. 3(2), pp. 311-317, 2011.
[47] Maria Ladar, Elisabeth-Jeanne Popovici, Ioan Baldea, Rodica Grecu, Emil Indrea, Journal of Alloys and Compound, vol. 434-435, pp. 697-700, 2007.
[48] V.Kumar , M.Saroja, M. Venkatachalam, S. Shankar, International Journal of ChemTech Research, vol. 6(6), pp. 3357-3360, 2014.
[49] Raghad Zein, Ibrahim Alghoraibi, International Journal of ChemTech Research, vol. 6(5), pp. 3220-3227, 2014.
[50] Ezenwa I.A. and Okoli N. L., European open Applied Physics Journal, vol. 1(1), pp. 1-9, 2015.
[51] Daniela E. Ortiz-Ramos, Luis A. Gonzalez, Rafael Ramirez-Bon, Materials Letters, vol. 124, pp. 267-270, 2014.
[52] Chao- Ming Huang, Lung- Chuan Chen, Guan- Ting Pan, C.K. Yang, Materials Chemistry and Physics, vol. 117, pp. 156-162, 2009.
[53] Baligh Touati, Abdelaziz Gassoumi, Salem Alfaify, Najoua Kamoun-Turki, Materials Sci. in Semiconductor Processing, vol. 34, pp. 82-87, 2015.
[54] P.P. Hankare, P.A. Chate, D.J. Sathe, A.A. Patil, Applied Surface Science, vol. 256, pp. 81-84, 2009.
[55] D. Johnston, I. Forbes, K.T. Ramkrishna reddy, R.W. Miles, J. of Mater. Sci. letters, vol. 20, pp. 921-923, 2001.
[56] P.A. Luque, Claudia M., Gomez-Gutierrez, G. Lastra, A. Carrillo-Castillo, M.A. Quevedo-Lopez, A. Olivas, Journal of Electronic materials, vol. 43(11), pp. 4317-4321, 2014.
[57] A.U. Ubale, D.K. Kulkarni, Bull. Mater. Sci., vol. 28(1), pp. 43-47, 2005.
[58] Ian Y.Y. Bu, Microelectronic Engineering, vol. 128, pp. 48-52, 2014.
[59] He-Jie Zhu, Xue-Mei Wang, Xiao-Yong Gao, Journal of the Korean Physical Society, vol. 67(2), pp. 366-370, 2015.
[60] C. Cruz-Vazquez, F. Rocha-Alonzo, S.E. Burruel-Ibarra, M. Barboza-Flores, R. Barnal, M. Inoue, Appl. Phys. A, vol. 79, pp. 1941-1945, 2004.
[61] Abdelhak Jrad, Tarek Ben Nasr, Najoua Turki-Kamoun, J Mater Sci.: Mater Electron, vol. 26(11), pp. 8854-8862, 2015.
[62] A.U. Ubale, V.S. Sangawar, and D.K. kulkarni, Bull. Mater. Sci., vol. 30(2), pp. 147-151, 2007.
[63] Heejin Ahn, Youngho Um, Journal of Korean Physical Soc., vol. 67(6), pp. 1045-1050, 2015.
[64] E.I. Anila, T.A. Safeera, R. Reshmi, J Fluoresc., vol. 25(2), pp. 227-230, 2015.
[65] Muhammad Saeed Akhtar, Mohammad Azad Malik, Saira Riaz, Shahzad Naseem, Paul O' Brien, Mater. Sci. in SemiCond. Processing, vol. 30, pp. 292 – 297, 2015.
[66] M.H. Doha, M.J. Alam, J. Rabeya, K.A.M.H. Siddiquee, S. Hussain, O. Isalam, M.A. Gafur, S. Isalam, Optik, vol. 126, pp. 5194-5199, 2015.
[67] G.L. Agawane, Seung Wook Shin, M.S. Kim, M.P. Suryawanshi, K.V. Gurav, A.V. Moholkar, J. Y. Lee, Current Appl. Phys., vol. 13, pp. 850-856, 2013.
[68] Huan Ke, Shuwang Duo, Tingzhi Liu, Qi Sun, Chengxiang Ruan, Xiaoyan Fei, Jilin Tan, Sheng Zhan, Mater. Sci. in Semicond. Processing, vol. 18, pp. 28-35, 2014.
[69] Seung wook Shin, G.L. Agawane, Myeng Gil Gang, A.V. Mohalkar, Jong-Ha Moon, Jin Hyeok Kim, Jeong Yong Lee, J. of alloys and Comp., vol. 526, 25-30, 2012.
[70] Aixiang Wei, Jun Liu, Mixue Zhuang and Yu Zhao, Mater. Sci. in Semicon. Processing, vol. 16, pp. 1478-1484, 2013.
[71] So Ra Kang, Seung Wook Shin, Doo Sun Choi, A.V. Moholkar, Jong-Ha Moon, Current Appl. Phys., vol. 10, pp. S473-S477, 2010.
[72] F. Gode, C. gumus, M.Zor, J. of Cryst. Growth, vol. 299, pp. 136-141, 2007.
[73] Seung Wook Shin, So Ra Kang, K.V. Gurav, Jae Ho Yun, Jong-Ha Moon, Jeong Yong Lee, Jin Hyeok Kim, Solar Energy, vol. 85, pp. 2903-2911, 2011.
[74] G.L. Agawane, Seung Wook Shin, A.V. Moholkar, K.V. Gurav, Jae Ho Yun, Jeong Yong Lee, Jin Hyeok Kim, J. of Alloys and compounds, vol. 535(15), pp. 53-61, 2012.
[75] P.A. Luque, A. Castro-Beltran, A.R. Vilchis-Nestor, M.A. Quevedo-Lopez, A. Olivas, Mater. Lett., vol. 140, pp. 148-150, 2015.
[76] Jun Liu, Aixiang Wei, Yu Zhao, J. of Alloys and Comp., vol. 588, pp. 228-234, 2014.
[77] Limei Zhou, Nan Tang and Sumei Wu, Surface & Coating Technol., vol. 228, pp. 146, 2013.
[78] Seung Wook Shin, So Ra Kang, Jae Ho Yun, A.V. Mohalkar, Jong-Ha Moon, Jeong Yong Lee, Jin Hyeok Kim, Solar Energy & Solar Cells, vol. 95, pp. 856-863, 2011.
[79] Qi Liu, Mao Guobing, Ao Jianping, Appl. Sur. Sci., vol. 254, pp. 5711-5714, 2008.
[80] Taisuke Iwashita, Shizutoshi Ando, Thin Solid Films, vol. 520, pp. 7076-7082, 2012.
[81] Meng Cao, Bin Lei Zhang, Jian Huang, Shou Ren Zhao, Hong Cao, Jin Chun Jiang, Yan Sun and Yue Shen, Mater. Res. Bull., vol. 48, pp. 357-361, 2013.
[82] Limei zhou, Nan Tang, Sumei Wu, Xiaofei Hu and Yuzhi Xue, Phys. Procedia, vol. 22, pp. 354-359, 2011.
[83] L.G. Sillen, A.F. Martell(Eds.), Stability Constant of Metal Ion Complexes, Special Publication, No. 25, The Chemistry Society London, 1971.
[84] M. Froment, D. Lincot, Electrochim. Acta, vol. 40, pp. 1293, 1995.
[85] S. Biswas, P. Pramanik, P.K. Basu, Mater. Lett., vol. 4(2), pp. 81-84, 1986.

[86] P.K. Nair, M.T.S. Nair, Semicond. Sci. Technol., vol. 7, pp. 239, 1992.
[87] I.C. Ndukwe, Solar Energy Mater. Solar Cells, vol. 40, pp. 123, 1996.
[88] B. Mokili, Y. Charreire, R. Cortes, D. Lincot, Thin Solid Films, vol. 288, pp. 21, 1996.
[89] G.A. Kitaev, A.A. Uritskaya, S.T. Moksushin, Russ. J. Phys. Chem., vol. 39, pp. 1101-1102, 1965.
[90] J.M. Dona, J. Herrero, J. Electochem. Soc., vol. 141, pp. 205, 1994.

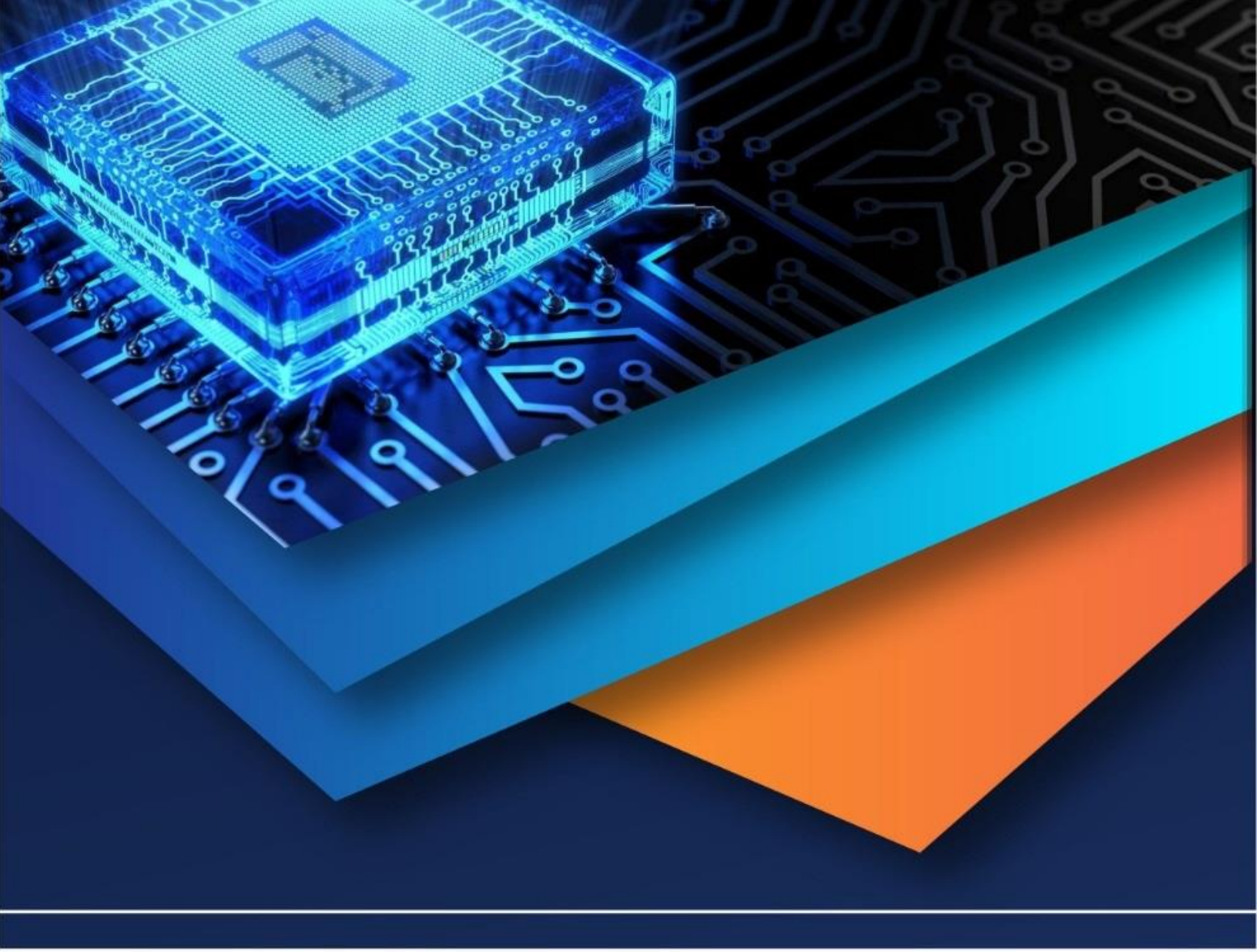

10.22214/IJRASET

45.98

IMPACT FACTOR: 7.129

IMPACT FACTOR: 7.429

INTERNATIONAL JOURNAL FOR RESEARCH

IN APPLIED SCIENCE & ENGINEERING TECHNOLOGY